ELSEVIER

Journal of Organometallic Chemistry 570 (1998) 225–234

Journal of Organometallic Chemistry

Theoretical study of electrophilic versus nucleophilic character of transition metal complexes of phosphinidene

Gilles Frison [a], François Mathey [b,*], Alain Sevin [a]

[a] *Laboratoire de Chimie Théorique, UMR 7616 Université Pierre et Marie Curie and CNRS, T-22-23, Case 137, 4 Place Jussieu, 75252 Paris Cedex 05, France*

[b] *Laboratoire Hétéroéléments et Coordination, URA 1499 CNRS, DCPH, Ecole Polytechnique, 91128 Palaiseau Cedex, France*

Received 17 April 1998

Abstract

A comparative theoretical study of the terminal phosphinidene complexes $HPCr(CO)_5$, $HPTi(Cp_2)$ and $HPTiCl_2$, at the MP2 and DFT levels, has been carried out. The calculated results have then been used for determining the electron localization function (ELF) in these moieties. Both techniques show that in the singlet ground state of $HPCr(CO)_5$, one gets a weak double P–Cr bond, with an electrophilic character on P (i.e. electron-deficient center). Conversely, in the singlet ground state of Ti complexes, the P–Ti bond shows a greater double bond character than in the P–Cr linkage, associated with an overall nucleophilic character of P. These results are in good agreement with all available experimental data. © 1998 Elsevier Science S.A. All rights reserved.

Keywords: Phosphinidene complexes; Electrophilic and nucleophilic behaviour; Electron localization function

1. Introduction

Up to now, free phosphinidenes PR, have only been observed as short-lived species in dilute gas phase or in matrices at low temperature [1]. Examination of the lowest energy triplet and singlet electronic configurations, schematically displayed for the prototype PH in Fig. 1, clearly reveals their analogy with carbenes. Indeed, both types of moieties are very reactive, and condensation reactions with a great variety of partners [2] as well as skeleton rearrangements [3] take place very readily as shown by both experimental and theoretical studies [4]. On the other hand, the formation of stable or transient η^1-transition metal complexes, which will be referred to as RPM(L) in the following sections, is well documented [5,6]. Depending on the nature of the metal and associated ligands, the chemical reactivity of these complexes exhibits a striking dichotomy. as illustrated in Fig. 2.

When M = Cr, Mo, W, and (L) = $(CO)_5$, an overall electrophilic behavior of the PR end is observed, (upper part of the figure) [5,7], while a nucleophilic behavior results when M = Zr and (L) = Cp_2 (lower part of the figure) [8]. The theoretical results available in literature are conflictory [9]. Though not established, an analogy has been proposed [10]: (i) between electrophilic complexes of phosphinidenes and Fischer carbenes; (ii) between nucleophilic complexes of phosphinidenes and Schrock carbenes [11]. The role of the metal and the ligands therefore remains worth being studied. We present here a theoretical study of the electronic properties of PH involved in two kinds of linkages, $HPCr(CO)_5$ and $HPTiCp_2$, which might be regarded as limiting model structures of the so-called electrophilic and nucleophilic reactivity, respectively. In the aim of facilitating further reactivity explorations, the replacement of the Cp ligands by Cl atoms has been examined, as well as the replacement of Ti by Zr. Our study has consisted in two distinct, although linked parts. At first, a quantum mechanical determination of structural

* Corresponding author. Tel.: +33 169 334079; fax: +33 169 333990.

0022-328X/98/$ - see front matter © 1998 Elsevier Science S.A. All rights reserved.
PII S0022-328X(98)00875-4

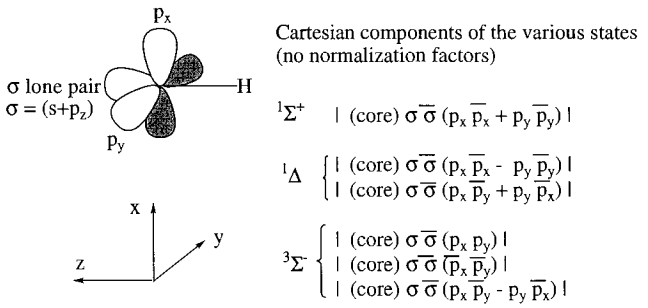

Fig. 1. Schematic display of the dominant electronic localization in the low-lying states of PH.

parameters, followed by analysis of the resulting electronic data has been carried out. In a second step, the results of these calculations have been used for calculating the associated electron localization functions (ELF), thus providing an original method for examining the changes in electronic densities as a function of the metal and the substituents.

2. Methodology

2.1. Quantum mechanical calculations

They have been performed with the GAUSSIAN 94 series of programs [12]. Owing to the large size of the systems under scrutiny, two limited basis sets have been selected. On one hand, the 3-21G [13] basis set has been used, either at the MP2 level of correlation or in DFT calculations, using the B3LYP scheme [14]. On the other hand, the LanL2DZ [15] basis set in which the inner shells are treated by pseudo-potential functions, has also been

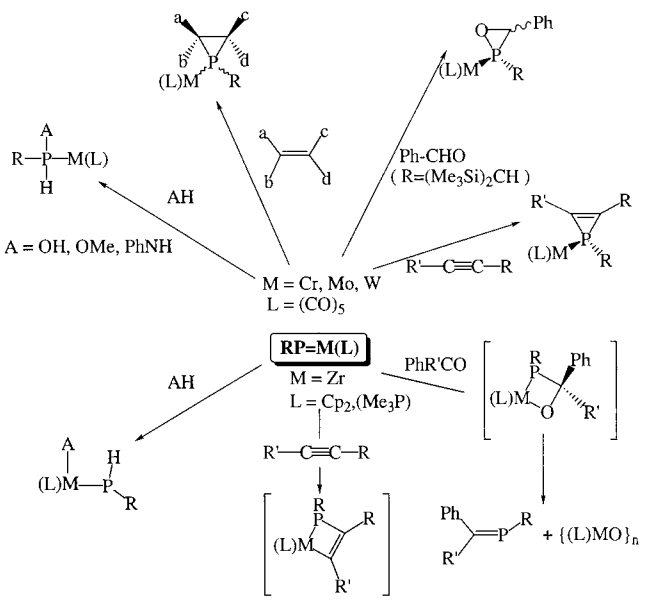

Fig. 2. Electrophilic (upper part) and nucleophilic (lower par) reactivities of the RPM(L) complexes as a function of the metal and ligands.

used, at both preceding levels of calculations. When dealing with $HPTiCl_2$, the more complete Ahlrichs' VTZ [16] basis set has been used at the DFT level. No striking difference between the so-obtained structural parameters and the previous ones has been found. This point, along with comparison with the available experimental data, vide infra, justifies to some extent the use of a limited basis set. In all cases the natural orbital population, either resulting from MP2 or DFT calculations, was used as the starting material for the determination of the ELF [17]. Technical details are given in the Appendix A.

3. Quantum mechanical study of isolated fragments: PH, $Cr(CO)_5$, $TiCp_2$

3.1. PH

Extended calculations on PH are available [4], and we will examine first the role of the basis set and the quantum method on the calculated structures and properties of the lowest energy singlet and triplet states. Typical results are reported in Table 1. It is noteworthy that all methods yield a triplet ground state (GS), in agreement with experiment [1]. We see that the 3-21G and LanL2DZ basis sets yield overestimated bond lengths, the deviation being $\sim 3\%$. When dealing with 3-21G results, the MP2 technique yields a singlet–triplet energy gap which is farther to the experimental value than the B3LYP one. At the same level of correlation, the VTZ basis set, as well as the 6–31G** yield similar results. Only the use of large basis sets together with extended correlation (last two entries), give data which might be compared to the experimental ones with less than 0.05% deviation for the PH bond length. Since, owing to the size of the systems, we had to preferentially use the B3LYP/3-21G, B3LYP/LanL2DZ or B3LYP/VTZ methods in the rest of this work, the relevant data show that: (i) the calculated PH bond lengths in complexes are likely to be slightly longer than actual ones in both types of calculations; (ii) the results obtained with the 3-21G basis set are more accurate than these obtained with the LanL2DZ basis set.

3.2. $Cr(CO)_5$

The GS of this species is a singlet of $^1A_1$ symmetry, corresponding to the d^6 $|(\text{core})(d_{xy})^2(d_{xz,yz})^4|$ electronic configuration, with the canonical axes of the C_{4v} point group. This result is in good agreement with previous calculations [18]. The optimized geometrical parameters are reported in Table 2. Once again we see that the LanL2DZ basis set yields bond lengths slightly longer than those obtained by other methods. It is noteworthy that all calculations reveal that the $Cr-C_{ax.}$ bond length is noticeably shorter than the $Cr-C_{eq.}$ one. The strong

Table 1
Experimental and calculated structures and energies of PH

Quantum method	Basis set	rP–H (Å)		E triplet[a]	ΔE_{ST} [b]
		Singlet	Triplet		
MP2	3–21G	1.455	1.458	−339.58419	40.08
MP2	LanL2DZ	1.461	1.464	−6.89424	41.27
B3LYP	3–21G	1.463	1.462	−340.15378	33.63
B3LYP	Ahlrichs VTZ	1.468	1.469	−341.89186	32.83
B3LYP	LanL2DZ	1.471	1.470	−7.02840	34.42
CASSCF(4,4)	3–21G	1.486	1.481	−339.57049	30.45
CASSCF(4,9)	3–21G	1.479	1.476	−339.57813	29.73
B3LYP	6–31G**	1.436	1.434	−341.87900	33.29
MCSCF [4]b	6–31G**	1.414	1.413	−341.26802	32.51
QCISD(T) [4]a	6–311++G(3df,2p)	1.415	1.414	−341.42402	28.00
Experiment [1]a		1.421	1.418		22.00

[a] Atomic units.
[b] Singlet–triplet separation, in kcal mol^{-1}.

axial bonding, in turn, is characterized by an important back-bonding reflected by the CO bond length, longer in the axial position than in the equatorial one.

3.3. $TiCp_2$

A sandwich D_{5h} structure yielding a $^3A_2'$ triplet GS, having the d^2 electronic configuration $|(\text{core})(d_{xy,x^2-y^2})^2|$ is obtained, as shown in Table 2. A similar result has been found in an extended Hückel theory (EHT) study by Hoffmann et al. [19].

4. Singlet and triplet $HPCr(CO)_5$

When dealing with this moiety, two types of stable electronic structures might be taken into account. In order to provide a simple explanation, let us consider the MO behavior, calculated at the EHT level, displayed in Fig. 3. This diagram has been obtained by fixing the geometrical parameters at their optimized value (see Table 2), and scanning the H–P–Cr angle (θ in Fig. 3). The dominant MO localizations are indicated in shorthand notation. Two limiting geometries are worth considering. (i) End-on coordination ($\theta = 180°$): in a linear Cr–P–H geometry, (right part), the σ lone pair of PH (see Fig. 1), interacts in a strong bonding fashion with the LUMO of $Cr(CO)_5$ and yields a stable σ-type Cr–P bond (not represented here) [20]. Through this interaction an electron transfer from PH to the metal takes place. The degenerate $3p_{x,y}$ set of PH AOs interact with the $3d_{xz,yz}$ MOs of $Cr(CO)_5$, in such a way that the degeneracy remains. A set of four π-type levels is obtained, composed of two bonding MOs (labelled π_x and π_y), and two antibonding MOs (labelled π_x^*, π_y^*). Both π and π^* MOs exhibit a strong mixing of Cr and P characters. These four MOs are filled by six electrons, as it is the case in O_2, or in the Fe^{IV}–O linkage of porphyrins [21]. The resulting triplet state bears an overall dominant covalent biradical character which may be regarded as the superposition of two 3-electron bonds, located in two orthogonal planes [22,23]. The latter result rules out the possibility for such a triplet state to account for observed electrophilic reactivity of the PH unit. (ii) Side-on coordination: upon bending of the PH bond, the preceding degeneracy is split, creating two types of MOs, of A' and A'' symmetry. The A'' set (π_y, π_y^* and d_{xy}) remains unchanged. The behavior of the A' MOs is more complex. Let us fix the H–P–Cr angle at 120° for the sake of discussion. In this geometry the low-energy σ lone pair MO and p_x on P yields two sp^2-type hybrids, one of which being able to coordinate via a σ-type bond to the metal, and the second one yields the P-lone pair which points out of the system (HOMO–3, Fig. 3). Accordingly, both π_x and π_x^* MOs are stabilized by two distinct effects: (a) π_x, through the introduction of s character coming from the hybridization of the P atom; (b) π_x^*, through the lowered antibonding interaction between d_{xz} and the P-lone pair. As an end result, the contributions of P increase in the bonding π_x MO, while the π_x^* MO becomes more concentrated on the metal. The essential feature is that this bonding scheme favours a singlet electronic configuration, contrary to the case of an end-on coordination.

To summarize this MO study, we see that two electronic configurations remain probable, a singlet one having a Cr–P–H angle close to 90°, and a triplet one with a Cr–P–H angle close to 180°. For intermediate geometries, these two states are predicted to remain close in energy.

4.1. Calculated results

The preceding MO analysis is comforted by the calculated results of Tables 3 and 4, where the data

Table 2
Calculated structures and energies of the parent complexes

Quantum method	Basis set	Cr–$C_{eq.}$[a]	Cr–$C_{ax.}$	C–$O_{eq.}$	C–$O_{ax.}$	E (au)
$Cr(CO)_5(C_{4v})$ $^1A_1$ singlet						
B3LYP	3-21G	1.872	1.788	1.167	1 172	−1603.04147
B3LYP	LanL2DZ	1.904	1.843	1.176	1.181	−652.90270
MP2 [18]		1.879	1.753	1.167	1.194	−651.90889
Quantum method	Basis set	Ti–C	Ti–Cp[b]	C–C	CH	E (au)
Cp_2Ti (D_{5h}) $^3A'_2$ triplet						
B3LYP	3-21G	2.385	2.052	1.430	1.080	−1230.37394
EHT [19]		2.32	1.996	1.39	1.1	

[a] All distances are in Å.
[b] Distance between Ti and the center of the Cp ring.

calculated for the eclipsed geometry of Fig. 3 are reported. The GS is a $^1A'$ singlet state (C_s point group) with a Cr–P–H angle of 103.4° and a Cr–P bond length of 2.332 Å. Only lying 5.46 kcal mol^{-1} above the singlet GS, one finds a $^3A''$ triplet state, with a longer Cr–P bond length of 2.402 Å and a Cr–P–H angle of 122.1° (Table 3). The calculated formation energy is −34.79 kcal mol^{-1}, in good agreement with the −38.1 kcal mol^{-1} value found in a previous study [9a]. This value lies in the range of usual simple bonds energies and does not deserve special comment due to the lack of comparative data with other types of phosphinidenes. In all types of calculations, the examination of the frontier MOs shows that the HOMO is concentrated on the metal while the LUMO is mostly localized on P. This result indicates that an electrophilic behavior of the PH moiety might be expected. Another type of argument comes from the analysis of the calculated Mulliken's charges. Though generally delicate to treat when dealing with transition metal complexes, their comparison might reveal interesting qualitative trends in the bonding pattern, as long as very similar structures are compared. When comparing the final singlet and triplet species to the isolated partners, two striking features emerge from the data of Table 4: (i) in the singlet state, the addition of a PH ligand decreases the positive charge on Cr, with respect to isolated $Cr(CO)_5$ fragment, and creates a partial weak positive charge on P (0.11); (ii) in the triplet state, the PH ligand is less an electron-donor than in the singlet state since the positive charge on Cr is higher (1.43 instead of 1.31), while the charge on P is very weakly negative (−0.02). In the triplet state, the spin density (α electrons), on P is 1.33 and 0.82 on Cr thus clearly showing the diradical character of this state.[1] In conclusion the singlet GS of $HPCr(CO)_5$ exhibits an electrophilic character mostly coming from σ donation of PH in the formation of the Cr–P bond. This mode of bonding is therefore not properly represented as a double bond due to the weak back-bonding actually observed. The presence of five CO ligands on the metal obviously plays a very important role since, to a large extent, they prevent effective back donation to PH. It might thus be anticipated that electron-donating ligands on Cr would possibly change or even reverse the actual electrophilic character of the P atom.

4.2. Conformation analysis of PH rotation around the Cr–P bond in the singlet state

The above stated result is consistent with the very low rotational barrier calculated for PH. With the B3LYP/3-21G method, one finds that the fully optimized bisected structure in which the PH group is located in one bisector plane of the xy axes[2] lies 0.24 kcal mol^{-1} below the eclipsed structure displayed in Table 3. This very weak energy difference is not significant at our level of calculation and we may say that PH rotation is practically free.

5. Singlet $HPTiCp_2$, $HPTiCl_2$ and $HPZrCl_2$

The main trends of the bonding pattern actually found in these species has already been qualitatively discussed, at the EHT level for $HPZrCp_2$ [24]. For the sake of simplicity, we have carried out EHT calculations on $HPTiCl_2$, shown in Fig. 4. Several important features emerging from both studies are worth considering. First of all, upon bending, no strong geometry

[1] In UHF calculations of open-shell species, the sum of all α spin densities is 2 in a triplet state, but might be locally higher than 2 due to compensating negative quantities, i.e. excess of β spin on other atoms.

[2] Structure in which the half-plane containing PH bisects the atom labelled C_2O_2–Cr–C_2O_2, while C_1O_1 stands for the axial ligand: Cr–P 2.328 Å; P–H 1.461 Å; Cr–C_1 1.871 Å; Cr–C_2 1.883 Å; Cr–C_3 1.890 Å; C_1–O_1 1.165 Å; C_2–O_2 1.165 Å; C_3–O_3 1.164 Å; Cr–P–H 102.5°.

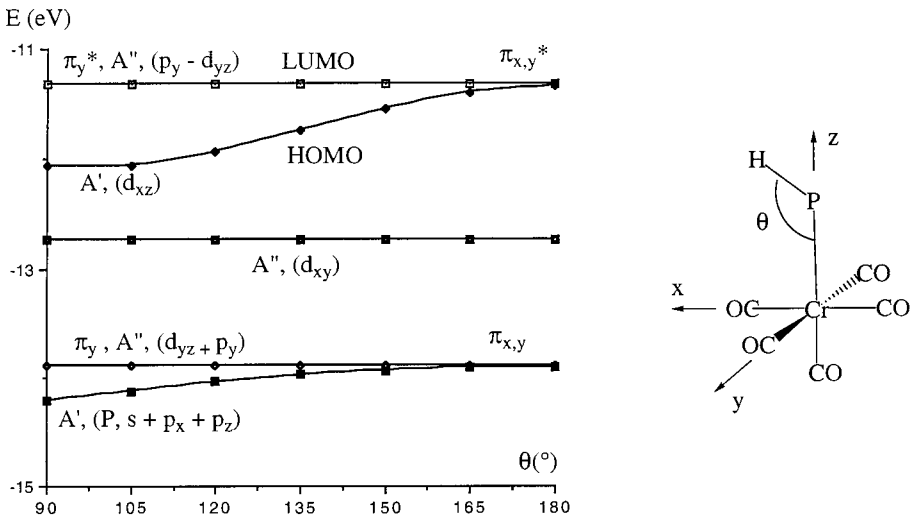

Fig. 3. MO correlation diagram (EHT) for $HPCr(CO)_5$. The dominant localization of the various MOs is indicated. The P–Cr σ-bonding MO which lies at lower energy is not represented here.

dependence is observed for the set of frontier MOs, contrary to the case of $HPCr(CO)_5$. This results from the fact that the frontier metal MOs are pushed up by interactions with the Cl or Cp ligands, and thus weakly interact with the P MOs or AOs. Apart from the σ-type P–Cr bonding MO, which is not represented here, one finds two MOs mostly localized on P: (i) π_y, of A'' symmetry, which is a mixture of p_y of P with a minor contribution of d_{yz}; (ii) the HOMO, of A' symmetry, which is composed of a mixture of $s + p_x + p_y$ (P-lone pair), with minor contributions of d_{xz}. These MOs yield a rather classical double bond character for the P–Ti linkage, with an overall nucleophilic character of the P atom. Moreover, it may be anticipated that the actual geometry mostly depends on steric interactions that are not adequately treated by this crude model study (vide infra). The calculated results are treated thereafter.

5.1. $HPTiCp_2$

The corresponding optimized geometry parameters and energies given in Table 5 have been obtained using the following strategy: (i) X_1 and X_2 being the centres of each cylopentadienyl ligand (Cp), a global C_{2v} structure was fixed, with P, Ti, X_1, X_2 located in the zx plane; (ii) each Cp was set perpendicular to its TiX axis, with the above CH eclipsing the Ti–P bond, so as to preserve the C_{2v} geometry; (iii) the PH bond was constrained to remain in the zx plane, yielding a global C_s geometry, as shown in the upper part of Table 5. All geometry parameters were optimized with these restrictions. The rotation of PH around the Ti–P axis has also been studied, showing that the eclipsed conformation with Ti–X_1 is optimal. It is noteworthy that both methods of calculation yield good comparable results, with Ti–P and PH bond lengths which are very similar to these calculated in singlet $HPCr(CO)_5$ (see Table 3). The Ti–P bonding energy, calculated at the B3LYP/3-21G level, is -45.83 kcal mol^{-1}, which is larger than when dealing with the Cr–P bond (-34.79 kcal mol^{-1}), thus leading to the assumption that the double bond character might be accentuated in this species, as previ-

Table 3
Calculated (B3LYP/3-21G) structural data and energies of singlet and triplet $HPCr(CO)_5$, in the eclipsed geometry

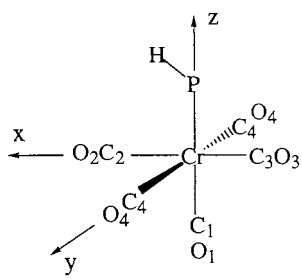

Singlet (eclipsed geometry)		Triplet (eclipsed geometry)
Energy (au) -1943.25069 Formation energy (kcal mol^{-1}) -34.79[a]		Relative energy (kcal mol^{-1}) 5.46
Cr–P	2.332	2.402
P–H	1.460	1.441
Cr–C_1	1.871	1.862
Cr–C_2	1.863	1.886
Cr–C_3	1.877	1.915
Cr–C_4	1.900	1.884
C_1–O_1	1.165	1.166
C_2–O_2	1.166	1.165
C_3–O_3	1.165	1.161
C_4–O_4	1.164	1.164
Cr–P–H	103.4°	122.1°

[a] With respect to the GS energies of fragments given in Table 2.

Table 4
Comparative calculated (B3LYP/3-21G) charges and spin densities of $HPCr(CO)_5$ and its constitutive fragments

	Charges[a]	Spin density
PH singlet		
P	0.05	
PH triplet		
P	0.06	2.07
$Cr(CO)_5$ singlet		
Cr	1.75	
$C_{ax.}$	−0.05	
$C_{eq.}$	0.04	
$O_{ax.}$	−0.40	
$O_{eq.}$	−0.37	
$HPCr(CO)_5$ singlet		
Cr	1.31	
P	0.11	
H	−0.04	
Cl	0.02	
C_2–C_4 [b]	0.10	
O_1	−0.36	
O_2–O_4 [b]	−0.36	
$HPCr(CO)_5$ triplet		
Cr	1.43	0.82
P	−0.02	1.33
H	0.00	0.00
Cl	0.01	−0.02
C_2–C_4 [b]	0.10	−0.03
O_1	−0.36	0.05
O_2–O_4 [b]	−0.36	0.01

All calculations have been carried out at the DFT/B3LYP/3–21G level
[a] Mulliken's charges.
[b] Average values.

ously stated in a study of Zr complexes of phosphinidenes by Stephan et al. [24]. The examination of the calculated MOs show that for all methods, contrary to the case of $HPCr(CO)_5$, the HOMO is mostly concentrated on the P atom, while the LUMO has dominant contributions localized on Ti. This finding nicely confirms the preceding EHT discussion. The comparison of the atomic charges calculated in the final singlet state with these of the isolated partners (Table 5, first column) shows a decrease of the negative charge on the Cps (−0.41 instead of −0.59) and an increase of the negative charge on P (−0.33 instead of 0.06). This confirms the nucleophilic character observed for this species and indicates that the π back-donation from Ti to P is larger in $HPTiCp_2$ than in $HPCrCO_5$.

5.2. Singlet $HPTiCl_2$ and $HPZrCl_2$

In this part, we will restrict ourselves to the study of the lowest energy singlet states, which are more stable than the corresponding triplet states.[3] A behavior very similar to that of $HPTiCp_2$ is observed for the two moieties, as shown in Table 5. A comparison of the structures in singlet $HPTiCp_2$ and $HPTiC1_2$ shows the strong similarity existing between both compounds. As previously noted in literature [25], the most important geometrical change consists in a 5% shortening of the M–P bond length when Cl substituents are present. The use of the VTZ basis set does not change these results significantly (Table 5, columns 3 and 4). The replacement of Ti by Zr does not bring important changes about, except for the Zr–P bond length which is larger in the Zr case, as expected. The calculated distance of 2.383 Å, increased by 5% (vide supra), might be compared to the experimental one of 2.505 Å which has been found in $Cp_2Zr(P(C_6H_2t\text{-}Bu_3))(PMe_3)$ [6]c. The aforementioned similarity is also illustrated when dealing with the frontier MOs, both HOMOs being concentrated on the P atom, and both LUMOs on Ti or Zr. It is worth recalling that the reverse trend has been found when dealing with $HPCr(CO)_5$ (vide supra). These results show that the replacement of Cp by Cl remains an interesting facility when large systems are to be studied and that, in both cases, the nucleophilic character of the PH entity is exalted by this type of complexation.

6. ELF comparative study of the singlet states of $HPCr(CO)_5$, $HPTiCp_2$, $HPTiCl_2$ and $HPZrCl_2$

In this part, attention is focused on the valence properties of the Cr–PH and Ti–PH linkages, without taking the core electronic populations of the metal atoms into account, which remain roughly constant with and without the PH ligand. The relevant data are given in Tables 5 and 6. For each species, the type of valence basin is precise, along with its calculated electronic population.

6.1. $HPCr(CO)_5$

Let us first examine the situation in which there is no bond between Cr and PH (separation 3.5 Å, entry 1, Table 6). One finds one disynaptic basin between P and H, corresponding to the actual PH bond, populated by 1.73 electron. Two monosynaptic basins are found on P, each with a mean population of 2.15 electrons, which represent the lone pair and the pair of singlet-coupled electrons born by the $3p_x$ and $3p_y$ AOs. The sum of these populations amounts to 6.03 electrons around the P atom, as expected, once the electron of H has been taken into account. When the PH unit is brought at the

[3] For $HPTiCl_2$, the calculated singlet–triplet energy gap is 9.90 kcal mol^{-1} (DFT/B3LYP/LanL2DZ).

optimal bonding distance (entry 2, Table 6), an important electronic redistribution takes place: (i) the disynaptic PH basin remains weakly affected; (ii) one monosynaptic basin with 2.53 electrons exists on P; (iii) two disynaptic basins are shared by Cr and P, with a total of 1.92 electron, revealing some character of a weak double bond; (iv) the total valence electrons found around P are 6.26. This result shows that the P atom does not drastically change its electronic population through complexation and the 0.23 electron difference with the non-bonded situation can be attributed to back-bonding from the Cr atom.

6.2. $HPTiCp_2$ and $HPTiCl_2$

The disynaptic V(P, H) basin of $HPTiCp_2$ (Table 5), is populated slightly less than in the previous case (1.69 instead of 1.80 electron), and two disynaptic basins are shared by P and Ti, with a total population of 2.16 electrons. The monosynaptic V(P) basin is populated by almost three electrons, leading to a total of 6.84 electrons around P. This value is higher than the above mentioned one (6.26), thus revealing an increase in nucleophilic character of the P atom. A similar situation is found when the Cps are replaced by Cl atoms, for which the total number of valence electrons located around P is 6.72. When dealing with $HPZrCl_2$, no important change is observed in the total valence electrons on P, (6.78 compared to 6.72 in $HPTiCl_2$), but the Zr–P linkage now involves 2.44 electrons, resulting from a stronger contribution of the P lone pair in the M–P bond, (2.69 electrons versus 2.96 in $HPTiCl_2$), rather than from a stronger back-bonding. The same result has been found in VTZ calculations. These results confirm the increased nucleophilic character with respect to $HPCr(CO)_5$.

7. Conclusion

Experimental studies on the reactivity of $RPM(CO)_5$ (with M = Cr, W) with alkenes and dienes have clearly established that these species have a reactivity similar to singlet electrophilic carbenes [26]. Indeed, retention of the alkene stereochemistry is observed during the formation of phosphirane complexes, and conjugated dienes were shown to give [2 + 1] cycloadducts, i.e μ^2-vinylphosphirane complexes. Additional kinetic data have shown that these species have an electrophilicity in the same range as that of alkylidene carbenes [27]. The analogy with existing between the PH unit in the complex, mostly composed of a σ-type lone pair (pointing out) and of an empty π-type AO (weak back-donation from Cr), and a free carbene, is fully supported by the theoretical results described here. The singlet state of $HPCr(CO)_5$ is found 5.46 kcal mol^{-1} below the corresponding triplet state. The ELF study indicates the presence of 6.26 electrons around P. The Cr–P bond can be considered as a weak double bond with 1.92 electrons between P and Cr and a bond length of 2.332 Å, which is precisely the sum of the covalent radii of Cr and P. The mild electrophilicity of P is corroborated by a positive charge of 0.11 on P in the singlet state.

In $HPTiCp_2$, the HOMO is mainly localized on P and the LUMO on Ti. The P–Ti bond energy is 45.83 kcal mol^{-1} versus 34.79 for P–Cr. The P atom is

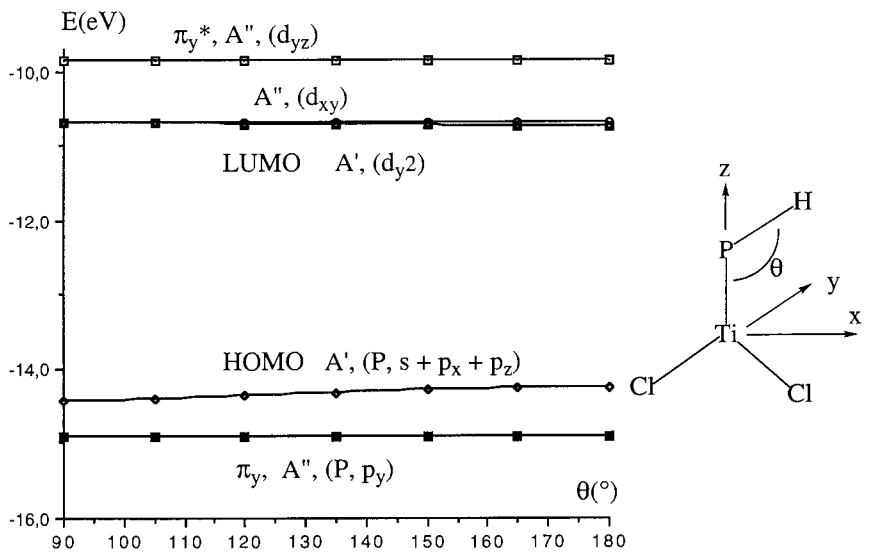

Fig. 4. MO correlation diagram (EHT) for $HPTiCl_2$. The dominant localization of the various MOs is indicated. The P–Ti σ-bonding MO which lies at lower energy is not represented here.

Table 5
Energies, structures, charges and ELF Population analysis of $HPTiCp_2$ $HPTiCl_2$ and $HPZrCl_2$

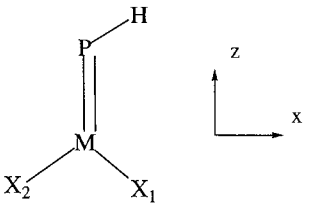

	M = Ti, X = Cp	M = Ti, X = Cp	M = Ti, X = Cl	M = Ti, X = Cl	M = Zr, X = Cl	Exp.[b]
Basis set	3-21G	LanL2DZ	LanL2DZ	Ahl. VTZ[(a)]	LanL2DZ	
Energy (au)	−1570.60074	−452.19593	−95.16953	−2111.97445	−83.68466	
Bondlengths (Å)						
P–M	2.325	2.348	2.239	2.230	2.383	2.505
P–H	1.453	1.457	1.455	1.436	1.458	
M–X[c]	2.051	2.085	2.229	2.240	2.408	
Angles (°)						
M–P–H	108.6	106.6	101.4	104.0	99.2	116.1
P–M–X_1	113.9	114.1	115.9	115.6	115.1	
P–M–X_2	107.3	106.9	110.3	109.9	108.5	
X–M–X	138.7	139.0	133.8	134.4	136.4	
Mulliken's charges[d]						
q(M)	1.25 (1.18)	0.13	0.62	0.97	0.70	
q(P)	−0.33 (0.06)	−0.09	−0.09	−0.28	−0.13	
q(H)	−0.09 (−0.06)	−0.08	0.01	0.02	0.00	
q(X)	−0.41 (−0.59)	0.00	−0.27	−0.36	−0.29	
Basin population (in electron)						
V(P, H)	1.69		1.67	1.74	1.66	
V(P, M)	1.08 × 2		1.05 × 2	1.19 × 2	1.22 × 2	
V(P)	2.99		2.96	2.69	2.69	
Total V	6.84		6.72	6.80	6.78	

All calculations have been carried out at the DFT/B3LYP level.
[a] Ahlrichs' VTZ basis set.
[b] $Cp_2Zr(P(C_6H_5t\text{-}Bu_3))$ (PMe_3) see Ref. [6]c.
[c] Mean value.
[d] The calculated values for the separate fragments PH and $TiCp_2$ are in parenthesis.

negatively charged (−0.33) and the ELF study indicates a population of 2.16 electrons in the P–Ti bond and 6.84 electrons around P. Thus, P is nucleophilic and the P–Ti bond shows a higher double bond character than the P–Cr bond, as in a true Schrock carbene.

Appendix A. ELF determination

The first approach in the field of electronic topology was made by Richard Bader in his theory of Atoms in Molecules, in which he applied topological concepts to the electronic density $\rho(\vec{r})$ [28]. More recently, the basis-independent ELF method, proposed by Becke and Edgecombe has proved to be very versatile in determining static and dynamic properties of electronic densities, in a great variety of molecules [29]. This function is:

$$\eta(\vec{r}) = \frac{1}{1 + \left(\frac{D(\vec{r})}{Dh(\vec{r})}\right)^2} \quad (1)$$

In this equation,

$$D(\vec{r}) = \frac{1}{2}\sum_i |\vec{\nabla}\phi_i(\vec{r})|^2 - \frac{1}{8}\frac{|\vec{\nabla}\rho(\vec{r})|^2}{\rho(\vec{r})} \quad (2)$$

is the excess of local kinetic energy density, due to Pauli repulsion [30].

$Dh(\vec{r}) = C_F\rho(\vec{r})^{5/3}$ is the Thomas–Fermi kinetic energy density which acts here as a renormalization factor, and C_F is the Fermi constant ($C_F = 2.871$ Å). The range of values of η is $0 \leq \eta \leq 1$. For a single pair of

Table 6
ELF population analysis of $HPCr(CO)_5$

System	Type of basin	Number of basins	Population by basin
$HPCr(CO)_5$	V(P, H)	1	1.73
(Cr–P = 3.5 Å)	V(P, Cr)	0	
	V(P)	2	2.15
			(Valence electrons on P: 6.03)
HPCr(CO)s	V(P, H)	1	1.80
(Optimized)	V(P, Cr)	2	0.96
	V(P)	1	2.53
			(Valence electrons on P: 6.26)

electrons with antiparallel spins, $\eta = 1$, while for the uniform gas of electrons, by construction $\eta = 0.5$. Recently, Silvi and Savin [31] applied these concepts to a new theory of bonding, in which a partition of the molecular space into basins of attractors having a clear signification is obtained. These basins are either core basins located around nuclei with $Z > 2$, or valence basins, some of which being associated with bonds. In this context, a classifications of bonds, has been proposed. The topological analysis has been performed with the TopMoD series of programs written in one of our laboratories [32]. These programs use as input the wfn file generated by GAUSSIAN 94, with natural orbital population. The calculations are then carried out in four steps: (i) evaluation of the ELF function over a 3D grid; (ii) identification of the various basins and assignment of the corresponding grid points; (iii) location of the critical points of the ELF function; (iv) integration of charge density over the basins.

References

[1] (a) P.F. Zittel, W.C. Lineberger, J. Chem. Phys. 65 (1976) 1236. (b) X. Li, S.I. Weissman, T.S. Lin, P.P. Gaspar, A.H. Cowley, A.I. Smirnov, J. Am. Chem. Soc. 116 (1994) 7899.

[2] (a) G. Fritz, T. Vaahs, H. Fleischer, E. Matern, Angew. Chem. Int. Ed. Engl. 28 (1989) 315. (b) G. Fritz, T. Vaahs, H. Fleischer, E. Matern, Z. Anorg. Allg. Chem. 570 (1989) 54. (c) X. Li, D. Lei, M.Y. Chiang, P.P. Gaspar, J. Am. Chem. Soc. 114 (1992) 8526.

[3] (a) A.H. Cowley, F. Gabbai, R. Scluter, D. Atwood, J. Am. Chem. Soc. 114 (1992) 3142. (b) S. Haber, P. Le Floch, F. Mathey, J. Chem. Soc., Chem. Commun. (1992) 1799.

[4] (a) M.T. Nguyen, A. Van Keer, L.G. Vanquickenborne, J. Org. Chem. 61 (1996) 7077. (b) P. Chaquin, A. Gherbi, J. Org. Chem. 58 (1993) 1379. (c) A. Sevin, A. Gherbi, P. Chaquin, Chem. Phys. Lett. 223 (1994) 237. (d) P. Chaquin, A. Gherbi, J. Org. Chem. 60 (1995) 3723. (e) P. Chaquin, A. Gherbi, D. Masure, A. Sevin, J. Mol. Struct. (Theochem.) 369 (1996) 85. (f) S.-J. Kim, T.P. Hamilton, H.F. Schaefer III, J. Chem. Phys. 97 (1993) 1872.

[5] F. Mathey, in: M. Regitz, O.J. Scherer (Eds.), Multiple Bonds and Low Coordination in Phosphorous Chemistry, Thieme, Stuttgart, 1990, p. 33.

[6] (a) A.H. Cowley, Acc. Chem. Res. 30 (1997) 445. (b) P.B. Hittchcock, H.F. Lappert, W.P. Leung, J. Chem. Soc., Chem. Commun. (1987) 1282. (c) Z. Hou, T.L. Breen, D.W. Stephan, Organometallics 12 (1993) 3158. (d) J.B. Bonnano, P.J. Wolczanski, E.B. Lobkorsky, J. Am. Chem. Soc. 116 (1994) 11159. (e) D.S.J. Arney, R.C. Schnabel, B.C. Scott, C.J. Burns, J. Am. Chem. Soc. 118 (1996) 6780.

[7] R. Streubel, A. Kusenberg, J. Jesjke, P.G. Jones, Angew. Chem. Int. Ed. Engl. 33 (1994) 2427.

[8] (a) T.L. Breen, D.W. Stephan, J. Am. Chem. Soc. 117 (1995) 11914. (b) T.L. Breen, D.W. Stephan, Organometallics 15 (1996) 4223. (c) T.L. Breen, D.W. Stephan, J. Am. Chem. Soc. 118 (1996) 4204.

[9] (a) J.-G. Lee, J.E. Boggs, A.H. Cowley, Polyhedron 5 (1986) 1027. (b) D. Gonbeau, G. Pfister-Guillauzo, A. Marinetti, F. Mathey, Inorg. Chem. 24 (1985) 4133.

[10] This analogy was first suggested in: S. Holland, F. Mathey, Organometallics 7 (1988) 1796 (Ref. 1).

[11] The dichotomy between Schrock and Fischer carbenes complexes has been rationalized from a theoretical stand point by: T.E. Taylor, M.B. Hall, J. Am. Chem. Soc. 106 (1984) 1576.

[12] M.J. Frisch, G.W. Trucks, H.B. Schlegel, P.M.W. Gill, B.G. Johnson, M.A. Robb, J. R. Cheeseman, T. Keith, G. A. Petersson, J. A. Montgomery, K. Raghavachari, M.A. Al-Laham, V.G. Zakrzewski, J.V. Ortiz, J.B. Foresman, J. Cioslowski, B.B. Stefanov, A. Nanayakkara, M. Challacombe, C.Y. Peng, P.Y. Ayala, W. Chen, M.W. Wong, J.L. Andres, E.S. Replogle, R. Gomperts, R.L. Martin, D.J. Fox, J.S. Binkley, D.J. Defrees, J. Baker, J.P. Stewart, M. Head-Gordon, C. Gonzalez, J.A. Pople, Gaussian 94, revision c.3. Gaussian Inc., Pittsburgh PA, 1995.

[13] (a) J.S. Binkley, J.A. Pople, W.J. Hehre, J. Am. Chem. Soc. 102 (1980) 939. (b) M.S. Gordon, J.S. Binkley, J.A. Pople, W.J. Pietro, W.J. Hehre, J. Am. Chem. Soc. 104 (1982) 2797.

[14] (a) A.D. Becke, J. Chem. Phys. 98 (1993) 5648. (b) P.J. Stephens, F.J. Devlin, C.F. Chabalowski, M.J. Frisch, J. Phys. Chem. 45 (1994) 98. (c) C. Lee, W. Yang, R.G. Parr, Phys. Rev. B 41 (1988) 785. (d) A.D. Becke, Phys. Rev. A 37 (1988) 785. (e) S.J. Vosko, L. Wilk, M. Nusair, Can. J. Phys. 58 (1980) 1200.

[15] (a) T.H. Dunning Jr., P.J. Hay, in: H.F. Schaefer, III (Ed.) Modern Theoretical Chemistry, Plenum, New York, 1976. (b) P.J. Hay, W.R. Wadt, J. Chem. Phys. 82 (1985) 270. (c) W.R. Wadt, P.J. Hay, J. Chem. Phys. 82 (1985) 284. (d) P.J. Hay, W.R. Wadt, J. Chem. Phys. 82 (1985) 299.

[16] A. Schäfer, H. Horn, R. Ahlrichs, J. Chem. Phys. 97 (1992) 2571.

[17] A. Savin, R. Nesper, S. Wengert, T.F. Fässler, Angew. Chem. Int. Ed. Engl. 36 (1997) 1808.

[18] A.W. Ehlers, G. Frenking, J. Am. Chem. Soc. 116 (1994) 1514.

[19] J.W. Lauher, R. Hoffmann, J. Am. Chem. Soc. 98 (1976) 1729.

[20] T.A. Albright, J. K. Burdett, M.H. Whangbo, Orbital Interactions in Chemistry, Wiley, New York, 1985 and references cited therein.

[21] A. Sevin, M.J. Fontecave, J. Am. Chem. Soc. 108 (1986) 3266.

[22] (a) L. Pauling, J. Am. Chem. Soc. 53 (1931) 3225. (b) M. Meot-Ner, Acc. Chem. Res. 110 (1984) 1672. (c) P.C. Hiberty, S. Humbel, P. Archirel, J. Phys. Chem. 98 (1994) 1169 and references cited therein.
[23] C. Dezarnaud-Dandine, A. Sevin, J. Am. Chem. Soc. 118 (1996) 4427.
[24] J. Ho, R. Rousseau, D.W. Stephan, Organometallics 13 (1994) 1918.
[25] M.T. Benson, T.R. Cundari, S.J. Lim, H.D. Nguyen, K. Pierce-Beaver, J. Am. Chem. Soc. 116 (1994) 3955.
[26] A. Marinetti, F. Mathey, Organometallics 3 (1984) 456.
[27] (a) K. Lammertsma, P. Chand, S.-W. Yang, T.T. Huang, Organometallics 7 (1988) 1875. (b) J.T. Huang, K. Lammertsma, Organometallics 11 (1992) 4365. (c) B. Wang, K. Lammerstma, J. Am. Chem. Soc. 116 (1994) 10486.
[28] R.F. Bader, Atoms in Molecules: A Quantum Theory, Oxford University Press, Oxford, 1990.
[29] A.D. Becke, K.E. Edgecombe, J. Chem. Phys. 92 (1990) 5397.
[30] A. Savin, J. Jepsen, O.K. Andersen, H. Preuss, H.G. von Schnering, Angew. Chem. Int. Ed. Engl. 31 (1992) 187.
[31] B. Silvi, A. Savin, Nature 271 (1994) 683.
[32] TopMoD, a series of programs written by S. Noury, X. Krokidis, F. Fuster, B. Silvi. This software is available upon request at the following e-mail address: xeno@lct.jussieu.fr